Exergy-based study of a binary Rankine cycle

Mathias Hofmann[a], George Tsatsaronis[b]

[a] *Institute for Energy Engineering, Technische Universität Berlin, Berlin, Germany, hofmann@iet.tu-berlin.de, CA*
[b] *Institute for Energy Engineering, Technische Universität Berlin, Berlin, Germany, tsatsaronis@iet.tu-berlin.de*

Abstract:

The aim of this work is to study a binary Rankine process with a significantly higher efficiency compared to a conventional coal-fired power plant. The paper focuses on the design of the process and especially on an efficient combination of flue gas, potassium and water streams in the components of the steam generator such as economizers, evaporators, superheaters, etc. to decrease the overall exergy destruction.
Based on a literature review, a base case for a coal-fired binary Rankine cycle with potassium and water as working fluids was developed and, in order to evaluate the thermodynamic quality of several variants, comparative exergy analyses were conducted.
A simulation of the process and calculation of the values for the streams was carried out by using the flow-sheeting program CycleTempo, which simultaneously solves the mass and energy balances and contains property functions for the specific enthalpy and entropy of all substances used. Necessary assumptions are predominantly based on literature data or they are discussed in the paper.
We present the exergy analysis of the overall process that includes the flue gas streams as well as the potassium and water subcycles. A design analysis and sensitivity studies show the effects of stream combinations and key parameters on the net efficiency, which is higher than 50 per cent.

Keywords:

Exergy Analysis, Binary Rankine Cycle, Liquid Metal Cycle, Potassium.

1 Introduction

Material limitations due to the combination of high temperatures and high pressures in supercritical coal-fired power plants do not allow a further significant raising of the working-fluid average thermodynamic-temperature during heat supply, so it will be difficult in the future to achieve a relevant increase of the thermodynamic efficiency. The availability of new, but more expensive materials for steam generators and turbines allows temperatures up to about 620 °C and pressures up to 300 bar, which results in a net efficiency of around 46 %.

In order to achieve a thermodynamic efficiency above 50 % for a coal-fired power plant, one or more topping cycles with suitable working fluids should be used. The principle of a binary Rankine cycle is shown in Fig. 1. The main idea is, connecting two Rankine cycles with a heat exchanger that acts as a condenser for the toping cycle and as an evaporator[1] for the bottoming cycle. As a result of the heat supply $\dot{Q}_{\mathrm{in}}$, the working fluid in the topping cycle will be heated and vaporized, see component A in Fig. 1. Potential sources of heat supply are combustion reactions, nuclear power or solar irradiation. We focus here on coal combustion. The maximum temperature of the working fluid in the topping cycle is T_2. The evaporation of the water in the bottoming cycle is a consequence of the condensation of the working fluid in component B in Fig. 1. In order to obtain superheated steam at temperature T_{c}, a further heat supply in component A is necessary.

This has already been proposed in the past and thermodynamic cycles with liquid metals were evaluated. So the first known ideas about binary Rankine cycles were published around one hundred years ago.

[1] Or also economiser, superheater etc.

In 1913, Emmet [1] introduced the “mercury-vapor process”. Extensive research work [2] led to the commercial operation of a plant with mercury as a working fluid in the topping cycle in 1928 [3]. Several other plants with a power output from 10 to 40 MW and net efficiencies of around 35 % were realized until the 1950s [4]. A further development of these systems was not pursued because of (a) the toxicity and the limited availability of mercury, (b) corrosion problems at higher temperatures, and (c) newer, more advanced conventional plants with a higher efficiency.

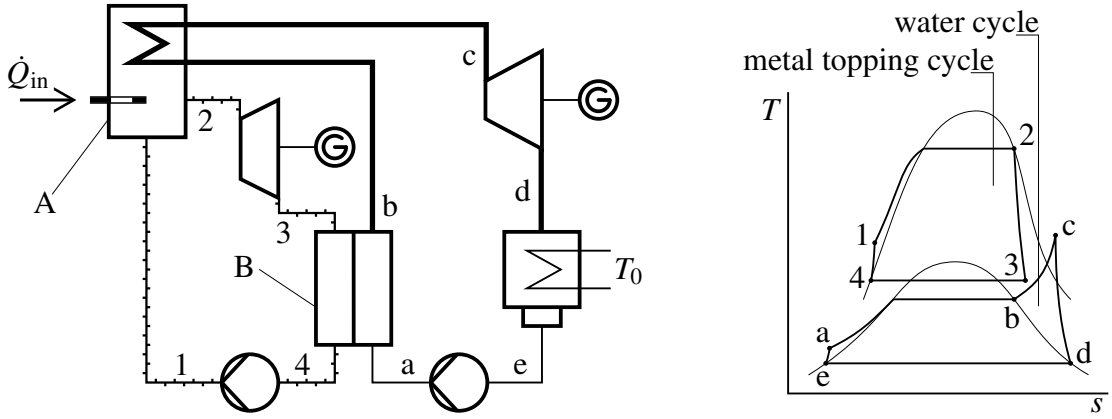

Fig. 1. Principle of a binary Rankine cycle with liquid metal as working fluid for the topping cycle, according to [5, p. 357]

In 1964, a research group led by Fraas at the ORNL developed a concept [6] for a binary Rankine cycle to be used for a stationary nuclear power plant with a molten salt reactor.[2] For their reference design with a reactor thermal output of 1000 MW, they indicated a net efficiency of 54.6 %.[3] They also discussed the search for a proper working fluid. They took into account factors such as material properties, availability and cost-effectiveness, and proved that particularly potassium was suitable. From todays point of view, this is still applicable. Their research was inspired by the development of efficient electrical space propulsion systems in the early 1960s. Zipkin and Schnetzer[4] [8] published a concept for a “nuclear electric one megawatt, two-phase, liquid metal system” and their group tested potassium turbine designs for several NASA programs[5]. At the same time, Ewing et al. [9] “measured several thermophysical properties” of the group Ia elements sodium, potassium and cesium as part of a “a property measurement program for the evaluation of several liquid metals as possible working fluids.” The thermodynamic properties[6] were widely used and republished for sodium and potassium e.g. in [10][7]. In 1974, Collier et al. [11] developed a concept for a helium-cooled nuclear reactor with potassium and water as working fluids for the Rankine cycles. For a reactor thermal output of 1570 MW, they calculated a net efficiency of 51 %.[8] In contrast to Fraas [6, 7], they changed the interconnections between the cycles. Half of the reactor output is released directly to the steam generator of the water cycle. Therefore, Collier et al. preferred a more parallel design, while Fraas promoted the serial design with the potassium condenser as the main interconnector between the Rankine cycles.

[2] Fraas [7] published another concept for an “oil-fired gas turbine potassium vapor-steam ternary cycle” in 1973.

[3] With the following temperature and pressure parameters. Topping cycle: potassium; saturated steam 838 °C, 2 bar; cold-end 593 °C, 0.165 bar. Bottoming cycle: water; superheated steam 566 °C, 276 bar; first reheat 566 °C, 72 bar; second reheat 566 °C, 17.3 bar; cold-end 46.1 °C, 0.0345 bar.

[4] Both General Electric.

[5] See, e.g. NASA reports under contracts NAS 3-8520, NAS 5-1143, NAS 3-10606, NAS 3-17354.

[6] Pressure, specific volume, temperature, specific enthalpy, specific entropy, specific heat.

[7] With a FORTRAN code to calculate the properties.

[8] With the following temperature and pressure parameters. Topping cycle: potassium; superheated steam, HP 930 °C, 2.07 bar; superheated steam, LP temperature N/A, 0.52 bar; cold-end 540 °C, 0.069 bar. Bottoming cycle: water; live steam 540 °C, pressure N/A; reheat 540 °C, pressure N/A; cold-end N/A.

Ganic and Seider [12] presented the results of a computer aided simulation in 1977, based on another suggestion by Fraas for a power plant with potassium as working fluid for the topping cycle and fluidized bed coal combustion. The net efficiency for a electrical output of 705 MW was given as 54 %.

Because of safety concerns related to a possible potassium-water reaction – caused by leakages in the potassium-condenser – Rajakovics [13] developed a ternary Rankine cycle[9] with potassium, biphenyl and water as working fluids in 1974. Until 1985, the idea was further developed and investigated under the IEA "Treble Rankine Cycle Project" funded by Germany, Netherlands and Austria. The results were published in [14]. Despite the high net efficiency for a coal-fired power plant of 51 % with an electrical output of 624 MW[10], the project was not pursued in this form. With the explanation in [15] that the biphenyl cycle is "very cost intensive" and "leak-free potassium/water heat exchangers are technically feasible without identifiable risk", they went back to the idea of binary Rankine cycles. Funded by the German government, a consortium of energy technology companies[11] further developed the concept of the binary Rankine cycle from 1986 until 1992, and published the results in [16, 17]. The process was designed with an electrical output of 316 MW, and therefore a net efficiency of 50 % could be determined.[12] In the year 1992, the electricity generation cost was approximately 10 % lower than for a conventional coal fired power plant[13]. The significant contributions of this study, especially concerning the potassium components[14], are also incorporated in the present work.

Contributions in the current literature deal with the selection of suitable working fluids and the determination of the efficiency of different process variants from a theoretical perspective. Angelino and Invernizzi [18] simulated binary Rankine cycles with different working fluids and recommended potassium for the topping cycle with a maximum process temperature of 850 °C. Components of the coal combustion and the flue gas system were not part of their simulations and they carried out only an energy analysis. Saunderson and Budiman [19] analyzed the efficiency of binary Rankine cycles with different combinations of several working fluids. According to their assumptions, the best possible combination would be mercury for the topping and ammonia for the bottoming cycle, with a maximum process temperature between 540 and 850 °C. Even if one neglected the toxicity and the limited availability of mercury, it must be noted that their conclusion stands in contradiction to the remark made by Fraas [7], that above 480 °C "corrosion of all types of steel by mercury made operation impractical."

Despite the numerous approaches in literature, so far there is no holistic view of the process with the aid of exergetic methods.

2 System Analysis

A base case for a coal-fired binary Rankine cycle with potassium and water as working fluids has been developed and a simulation of the process as well as calculation of the values for the streams have been carried out by using the flow-sheeting program CycleTempo [20], which simultaneously solves the mass and energy balances and contains property functions for the calculation of the specific enthalpy and entropy of all substances used. Necessary assumptions are shown in section 2.2 and in section 2.3 the methodology of the parameter as well as exergy analysis are presented. Finally the results are summarized in section 3.

[9] Also known as treble Rankine cycle (TRC).

[10] With the following temperature and pressure parameters. Topping cycle: potassium; saturated steam 870 °C, 2.6 bar; cold-end 477 °C, 0.026 bar. Intermediate cycle: biphenyl; saturated steam 455 °C, 20.8 bar; cold-end 287 °C, 1.45 bar. Bottoming cycle: water; saturated steam 270 °C, 55 bar; reheat 270 °C, 8 bar; cold-end 33 °C, 0.05 bar.

[11] Siemens (KWU), Babcock, Interatom, Balcke-Dürr etc.

[12] With the following temperature and pressure parameters. Topping cycle: potassium; saturated steam 850 °C, 2.24 bar; cold-end 521 °C, 0.06 bar. Bottoming cycle: water; superheated steam 545 °C, 215 bar; reheat 545 °C, 36 bar; cold-end 29.8 °C, 0.042 bar.

[13] $\eta_{net} = 37\,\%$

[14] Steam generator, turbine and condenser.

2.1 Process description and main parameters

Figure 2 shows the flow diagram for the simulation of the process. In order to simplify the illustration, we omitted detailed figures for the potassium steam turbine and lower level components like throttling valves. These components are considered in the exergy analysis. The meaning of all abbreviations can be found in the nomenclature. Ambient air enters the process via the FD-FAN and is preheated in a regenerative (APH1, Ljungstrom) and a recuperative air preheater (APH2, tubular). The coal is burned under a constant air ratio $\lambda = 1.25$ in the combustion chamber (CC).[15] The flue gas stream is used to heat up and vaporize the potassium in the economizer (K-FG-ECO) and evaporator (K-FG-EVAP).[16] The flue gas stream can be used either to heat up, vaporize or superheat the water. Alternatively, the potassium stream is used for that. Table 1 shows the options for the heat exchangers in the parameter analysis. All heat exchangers are counter flow heat exchangers, with the exception of K-FG-EVAP and W-K-EVAP, which are parallel flow heat exchangers.

Table 1. Options for the heat exchangers

Application	Primary option	Secondary option
heat up	56 W-K-ECO	48 W-FG-ECO
evaporate	55 W-K-EVAP	42 W-FG-EVAP
superheat	46 W-FG-SH1	53 W-K-SH1
	44 W-FG-SH2	51 W-K-SH2
reheat	47 W-FG-RH1	54 W-K-RH1
	45 W-FG-RH2	52 W-K-RH2

The saturated steam and cold-end parameters of the potassium cycle are constant and were chosen based on [15]. The potassium enters the turbine as saturated steam with 850 °C and 2.24 bar. The turbine is simulated with six stages. In order to avoid a quality x lower than 0.92, a turbine drainage is provided in accordance with [15]. Practically, a minimum quality of 0.87 is possible [11]. The main stream leaves the turbine with 523 °C and 0.06 bar and enters the main condenser (W-K-EVAP), where the water is vaporized. Optionally, the stream can be used with the same parameters in the economizer (W-K-ECO), the superheater (W-K-SH1) or the reheater (W-K-RH1). A side stream can leave the potassium turbine with higher temperature and pressure, to supply the superheater (W-K-SH2) and reheater (W-K-RH2). The fully throttled and condensed potassium enters the electromagnetic pump with 520 °C and 0.06 bar. The necessary delivery head is given by the pressure drops in K-FG-EVAP and K-FG-ECO, see Table 3.

In the bottoming cycle, the superheated steam flows to the high pressure water turbine (W-HPT) with 260 bar and to the intermediate pressure turbine (W-IPT) with 45 bar after being reheated. The superheated steam and reheated temperature are variable for the parameter analysis. Based on the ambient conditions, the given temperature rise of the cooling water and the minimum temperature difference, the pressure in the condenser (COND) is 0.065 bar; see also section 2.2. To increase the efficiency of the steam cycle, a regenerative feedwater heating with five low-pressure preheaters and a feedwater tank / dearator as well as three high-pressure preheaters and a desuperheater are included. For the flue gas purification, the selective catalytic reduction is designed as high dust process with an inlet temperature of around 380 °C and an assumed temperature drop of 30 K. The inlet temperature of the electrostatic percipitator (ESP) is 140 °C. After the flue gas desulfurisation (FGD), the clean gas flows to the stack with 50 °C.

[15] In the simulation, the complete ash is removed in the combustion chamber. In reality the main part (80 %) is removed in the electrostatic precipitator. For a typical ash mass balance of a dust-fired steam generator see [21, pp. 308]. We assume an ash temperature of 350 °C.

[16] The maximum temperature of potassium in K-FG-EVAP is 885 °C; for further information concerning the design of the potassium steam generator see [15].

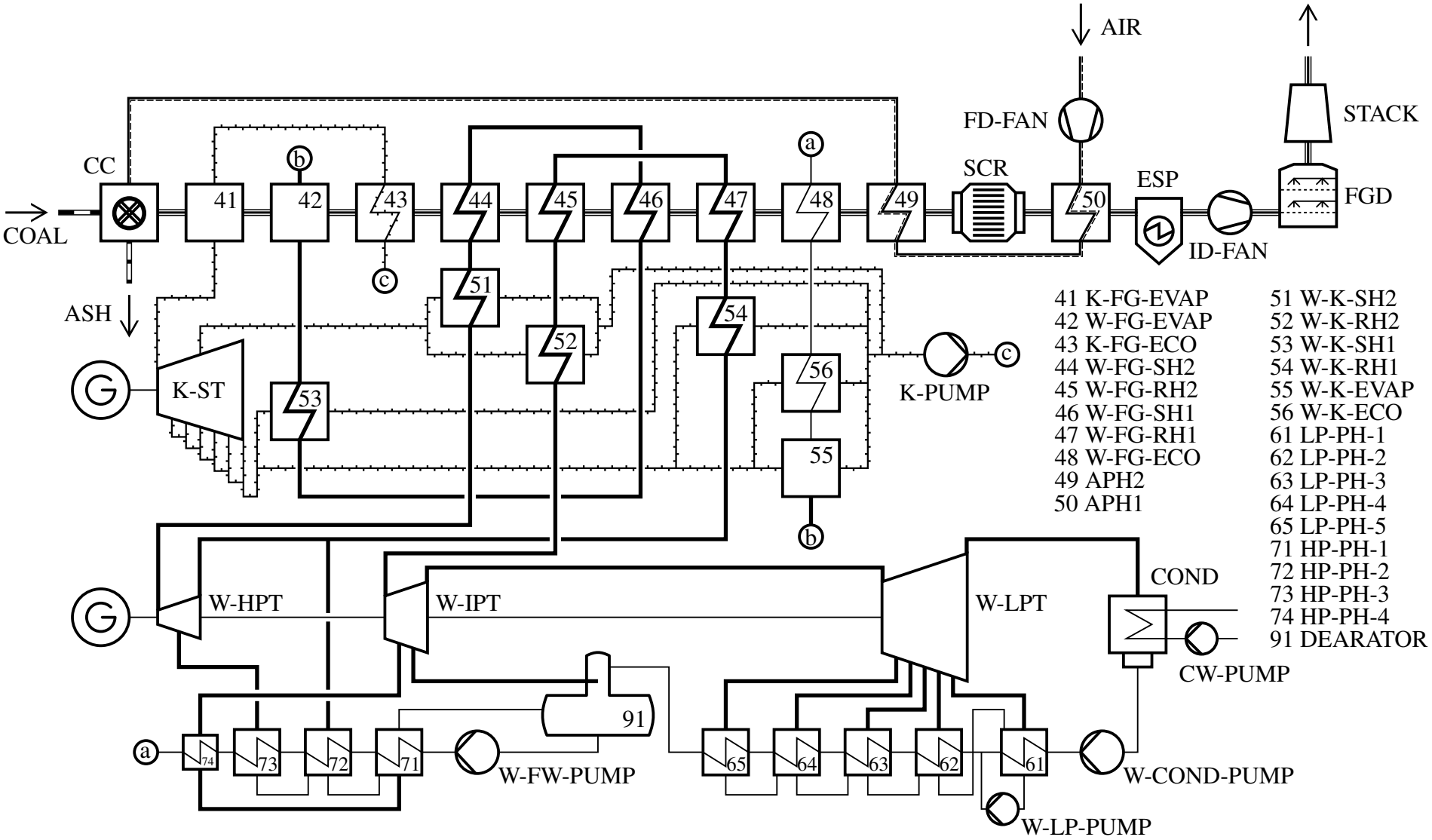

Fig. 2. Simplified flow diagram of the simulated coal-fired binary Rankine cycle with potassium and water as working fluids

2.2 Assumptions, simplifications and further specifications

The process is simulated at steady state. Changes in potential and kinetic energies are neglected and there are no heat losses over the surface of the components. Cycle and cooling water are treated as pure; properties are calculated with IAPWS97 formulations. The properties for potassium provided by Ewing [9] and Foust [10] are included in CycleTempo. There are no changes of the specific chemical exergies in the closed loops, since pure fluids are used (potassium, water, cooling water), therefore, only the differences of specific physical exergies are considered.

The ambient conditions T_0 and p_0 are valid for air, coal and cooling water and set to 25 °C and 1.013 bar. Both compositions, of air and coal, are given in Table 2. The composition of air is provided as *standard air* by CycleTempo. The composition of coal is given by [17, p. 31] with a lower heating value $LHV_{\text{coal}} = 27.6\,\text{MJ/kg}$. The chemical exergy for coal $e^{\text{CH}}_{\text{coal}} = 29.457\,\text{MJ/kg}$ has been calculated based on Eisermann's equations [22] and Szargut's standard chemical exergies [23, pp. 489]. To maintain a constant exergy rate of fuel, the mass flow of coal is fixed and the assumed value is 20 kg/s.

Table 2. Composition of Coal and Air

Coal components	ξ [kg/kg]	x [mol/mol]	Air components	x [mol/mol]
C	0.7094	0.6708	N_2	0.7661
H	0.0405	0.2283	O_2	0.2056
O	0.0612	0.0217	H_2O	0.0188
N	0.0118	0.0047	CO_2	0.0003
S	0.0071	0.0025	Ar	0.0092
Ash, SiO_2	0.0800	0.0151		
Water, H_2O	0.0900	0.0567		

For the heat exchangers we specify the exit temperature of the primary side, the minimum temperature difference as well as the pressure drops. The values are given in Table 3. The temperatures not given result (res) from mass and energy balances or they represent a degree of freedom (dof) in the parameter analysis. The typically low secondary pressure drops (flue gas side) in the heat exchangers of the steam generator are neglected (neg). The pressure drop of the primary side of the air preheaters is 20 mbar and 10 mbar for the secondary side. For the three components of the gas cleanup equipment the pressure drop is 10 mbar each. The required power of FD and ID-fan results from the pressure drops. The profile is illustrated in Fig. 3.

Table 3. Specifications for the heat exchangers

Heat exchanger	$T_{\text{e,prim}}$ [°C]	ΔT_{min} [K]	Δp_{prim} [bar]	Δp_{sec} [bar]
K-FG-EVAP	850	75	0.75	neg
K-FG-ECO	res	res	4.71	neg
All SH and RH[17]	dof	res	2.5 (each)	neg
W-K-EVAP, W-FG-EVAP	440	res	4 (each)	neg
W-K-ECO, W-FG-ECO	330	res	2.5 (each)	neg
HP-PH-*n*	res	5	2	neg
LP-PH-*n*	res	3	1.5	neg
COND	res	2.5	neg	neg
APH1	res	70	0.02	0.01
APH2	dof	70	0.02	0.01

Pressure drops for condensed mediums are also neglected and the pressure drops of the secondary side of heat exchangers like HP-PH can be neglected, because the stream is throttled to the next pressure level. For the exergy analysis the heat exchanger and the corresponding throttling valve were considered together.

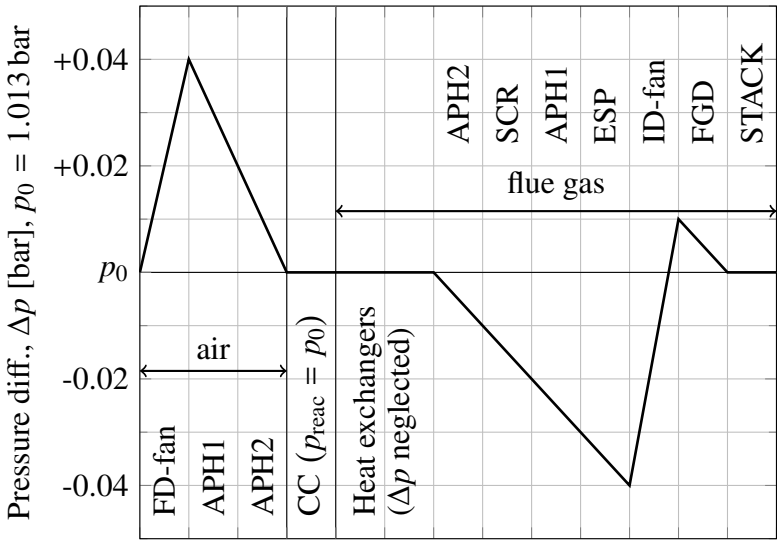

Fig. 3. Pressure profile of air and flue gas streams through steam generator, according to [24, p. 6-36]

The electrical work rate for a stage of a rotating equipment component is the product of the mass flow rate $\dot{m}$, the enthalpy difference for the isentropic process Δh_s and the isentropic efficiency η_s as well as the mechanical and electrical efficiency $\eta_{\mathrm{m,el}}$. With the parameter α as an indicator for the type.

$$\dot{W}_{\mathrm{el}} = \dot{m} \cdot \Delta h_s \left(\eta_{\mathrm{m,el}} \cdot \eta_s\right)^{\alpha} \qquad \alpha = \begin{cases} 1 & \text{turbines} \\ -1 & \text{pumps, fans} \end{cases} \tag{1}$$

The values for the isentropic efficiencies are based on literature data and are listed in Table 4. The mechanical efficiency η_{m} of all turbines are set to 99,5 %. The efficiencies of the generators η_{el} are set to 0.98. The efficiencies for the pumps or fans include the mechanical efficiencies of the pumps or fans, and the mechanical and electrical efficiencies of the motors are a function[18] of the work rate of the pump or fan. The delivery head of the cooling water pump is 15 m.

Table 4. Isentropic efficiencies of turbines, pumps and fans

Component	Isentropic efficiency η_s	Source, comment
K-ST-1…K-ST-6	0.90	[16, p. 85]
W-HPT / W-IPT / W-LPT	0.90 / 0.91 / 0.88	ibid. and [5, p. 247]
K-PUMP	3 kW if $\dot{m} = 1\,\mathrm{kg/s}$ & $\Delta p = 7.8$ bar	[15], electromagnetic
W-FW-PUMP, W-COND-PUMP	0.84	[5, p. 248]
W-LP-PUMP	0.80	ibid.
CW-PUMP	0.82	ibid.
FD-FAN, ID-FAN	0.83	ibid.

[17] W-FG-SH1, W-FG-SH2, W-FG-RH1, W-FG-RH2, W-K-SH1, W-K-SH2, W-K-RH1, W-K-RH2

[18] Given by CycleTempo. For the typical work rate between 1 and 5 MW like cooling water pump, feed water pump or fans we have $\eta_{\mathrm{m,el}} \approx 0.95$.

2.3 Parameter and exergy analysis

For the system analysis three cases are considered, where the primary exit temperature of the heat exchangers listed in Table 5 was varied. With these values we can show the influence of combinations of streams and key parameters on the net efficiency. The reference case essentially based on the concept presented by Lojewski et al. [15]. In case 1 and 2 a side stream from the potassium turbine is used to supplant a part of the thermal power of the flue gas for superheat and reheat. Consequently we have a higher inlet temperature of the flue gas in APH2 and thus a higher exit temperature at the air side.

Table 5. Primary exit temperature in the heat exchangers for the parameter analysis

Heat exchanger	Reference	Case 1	Case 2
		$T_{\mathrm{e,prim}}$ [°C]	
K-FG-ECO	598	770	814
W-FG-SH1	480	/	/
W-FG-SH2	545	500	510
W-K-SH2	/	545	570
W-FG-RH1	380	/	/
W-FG-RH2	545	460	510
W-K-RH2	/	545	570
APH2	290	430	430

In order to evaluate the thermodynamic quality of several options, comparative exergy analyses are conducted. As results from the simulation we obtain the mass flow, the specific enthalpies and entropies and the composition of all streams. Using the equations from Bejan et al. [25] the physical, chemical and total exergies of all streams are calculated.

The overall exergy balance is written with the net power output $\dot{W}_{\mathrm{net}}$ as exergetic product. The overall exergetic loss $\dot{E}_{\mathrm{L,tot}}$ is the sum of the losses over the stack, the ash and cooling water.

$$\dot{E}_{\mathrm{P,tot}} = \dot{W}_{\mathrm{net}} = \dot{E}_{\mathrm{F,tot}} - \dot{E}_{\mathrm{D,tot}} - \dot{E}_{\mathrm{L,tot}} \tag{2}$$

For the overall process we define the net efficiency based at the lower heating value and the exergetic efficiency shown in (3). The exergetic fuel for the overall process $\dot{E}_{\mathrm{F,tot}}$ is the chemical exergy of the coal stream only, because the temperature and pressure of coal and air are T_0 and p_0 respectively, and air is a part of the environment. No other streams enter the process.

$$\eta_{\mathrm{net}} = \frac{\dot{W}_{\mathrm{net}}}{\dot{m}_{\mathrm{coal}} \cdot LHV_{\mathrm{coal}}} \qquad \epsilon_{\mathrm{tot}} = \frac{\dot{W}_{\mathrm{net}}}{\dot{m}_{\mathrm{coal}} \cdot e^{\mathrm{CH}}_{\mathrm{coal}}} \tag{3}$$

For the kth component we calculate the exergy destruction rate based on the entropy generation. The definition of the exergy destruction ratio and the exergy loss ratio are also shown in (4).

$$\dot{E}_{\mathrm{D},k} = T_0 \cdot \dot{S}_{\mathrm{gen},k} \qquad y^*_{\mathrm{D},k} = \frac{\dot{E}_{\mathrm{D},k}}{\dot{E}_{\mathrm{D,tot}}} \qquad y_{\mathrm{L}} = \frac{\dot{E}_{\mathrm{L}}}{\dot{E}_{\mathrm{F,tot}}} \tag{4}$$

3 Results

The summarized results are shown in Table 6. In the reference case the net efficiency is 50 % for the overall process. That corresponds to the outcomes of Lojeweski et al. [15]. For case 1 the net amount of power increases by 3.5 MW while the total exergy destruction rate decreases by 7.3 MW. That results in a net efficiency of 50.7 %. A further increase of the net amount of power and a further decrease of

the total exergy destruction rate are realized in case 2. The net efficiency rises to 51.1 %. The reasons for the changes can be described using the results for the component-specific exergy destruction rates[19] in Table 6.

Table 6. Results of the exergy-based parameter analysis

	Reference		Case 1		Case 2	
Overall process[20]	$\frac{\dot{m}_\mathrm{K}}{\dot{m}_\mathrm{W}}$ [-]	0.92	$\frac{\dot{m}_\mathrm{K}}{\dot{m}_\mathrm{W}}$ [-]	1.13	$\frac{\dot{m}_\mathrm{K}}{\dot{m}_\mathrm{W}}$ [-]	1.19
	$\frac{\dot{W}_\mathrm{el,K}}{\dot{W}_\mathrm{el,W}}$ [-]	0.41	$\frac{\dot{W}_\mathrm{el,K}}{\dot{W}_\mathrm{el,W}}$ [-]	0.49	$\frac{\dot{W}_\mathrm{el,K}}{\dot{W}_\mathrm{el,W}}$ [-]	0.49
	$\dot{W}_\mathrm{net}$	276.21	$\Delta\dot{W}_\mathrm{net}$	+3.47	$\Delta\dot{W}_\mathrm{net}$	+5.63
	$\dot{E}_\mathrm{D,tot}$	284.74	$\Delta\dot{E}_\mathrm{D,tot}$	−7.29	$\Delta\dot{E}_\mathrm{D,tot}$	−9.39
	$\dot{E}_\mathrm{L,tot}$	28.20	$\Delta\dot{E}_\mathrm{L,tot}$	+3.82	$\Delta\dot{E}_\mathrm{L,tot}$	+3.77
	$\dot{E}_\mathrm{F,tot}$	589.15	$\Delta\dot{E}_\mathrm{F,tot}$	±0	$\Delta\dot{E}_\mathrm{F,tot}$	±0
η_net [%]	50.04		50.67		51.06	
ϵ_tot [%]	46.88		47.47		47.84	
Component[21]	$\dot{E}_{\mathrm{D},k}$	$y^*_{\mathrm{D},k}$ [%]	$\dot{E}_{\mathrm{D},k}$	$\Delta\dot{E}_{\mathrm{D},k}$	$\dot{E}_{\mathrm{D},k}$	$\Delta\dot{E}_{\mathrm{D},k}$
CC	153.74	53.99	141.72	−12.02	141.72	−12.02
K-FG-EVAP	30.84	10.83	33.99	+3.14	33.89	+3.05
W-HPT, W-IPT, W-LPT	22.48	7.90	21.50	−0.98	21.41	−1.07
W-EVAP (42, 55)	18.24	6.40	17.44	−0.80	16.70	−1.53
W-RH (45, 47, 52, 54)	10.31	3.62	9.58	−0.74	8.81	−1.50
APH1, APH2	10.03	3.52	12.32	+2.30	12.32	+2.30
SCR, ESP, FGD	9.97	3.50	9.96	−0.01	9.96	−0.01
W-SH (44, 46, 51, 53)	7.43	2.61	6.53	−0.90	5.78	−1.65
K-ST-1…K-ST-6	5.43	1.91	6.21	+0.78	6.22	+0.79
COND	5.31	1.86	5.08	−0.23	5.01	−0.30
HP-PH (71-74)	2.86	1.01	3.47	+0.60	3.80	+0.94
W-ECO (48, 56)	2.64	0.93	2.74	+0.09	2.64	±0
LP-PH (61-65, 91)	2.50	0.88	2.39	−0.11	2.41	−0.08
PUMP, FAN	1.97	0.69	1.97	−0.01	1.94	−0.03
K-FG-ECO	0.98	0.34	2.57	+1.59	2.69	+1.71
	$\dot{E}_\mathrm{L}$	y_L [%]	$\dot{E}_\mathrm{L}$	$\Delta\dot{E}_\mathrm{L}$	$\dot{E}_\mathrm{L}$	$\Delta\dot{E}_\mathrm{L}$
STACK	23.62	4.01	27.63	+4.01	27.63	+4.01
CW-SINK	4.36	0.74	4.17	−0.19	4.11	−0.24
ASH	0.22	0.04	0.22	±0	0.22	±0

As might be expected, the exergy destruction rate in the combustion chamber is more than half of the total exergy destruction rate. So one well known improvement strategy is to increase the air inlet temperature. That is realized in cases 1 and 2 with the expected effect, that the exergy destruction rate decreases in the combustion chamber and increases in the air preheaters. The higher temperature can be realized, because a condensed potassium stream is used to substitute a part of the heat supply by flue gas. The flue gas driven potassium evaporator K-FG-EVAP is one of the main heat exchangers in the steam generator. Here, the change of the exergy destruction rate is caused by the increase of the

[19] Due to the marginal change of the exergy destruction rates in the components SCR, ESP, FGD, COND, HP-PH, W-ECO, LP-PH, PUMP and FAN, these are not discussed in the comparative exergy analysis.

[20] If not given, dimension of data is [MW]. Differences relate to the reference case.

[21] In some cases several components are summarized. For the component numbers in parentheses see Fig. 2.

potassium mass flow and the higher inlet temperature of the primary side, where the mass flow has the decisive influence. The increase of the potassium inlet temperature for K-FG-EVAP substantially affects the exergy destruction rate in the potassium economizer K-FG-ECO. When comparing the contribution of the potassium and the water turbine stages to the overall exergy destruction rate, we note that the exergy destruction rate within the water turbines is around four times higher than within the potassium turbines. Two reasons for this can be indicated. First, the mass flow rates and the assumed isentropic efficiencies are nearly identical, see Tables 4 and 6. But the higher specific work of the water turbine stages[22] yields automatically to a higher entropy generation rate. Second, as mentioned by Bejan et al. [25, p. 147] "the rate of exergy destruction associated with friction varies directly with the head loss and inversely with the temperature level". The latter is higher in the potassium turbine, which yields to a higher exergetic efficiency there.[23] Hence, another improvement strategy is to increase the work rate of the potassium turbine, which is a general conclusion for topping cycles.

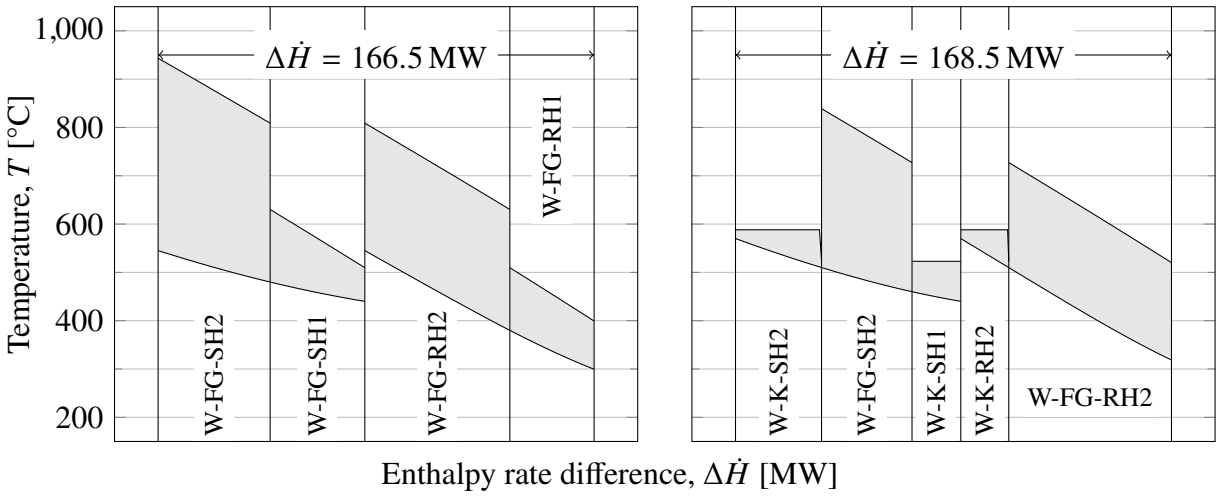

Fig. 4. $T,\Delta\dot{H}$-Diagramm for selected heat exchangers, left: Reference, right: Case 2

The secondary option for the potassium driven water evaporator W-K-EVAP – see Table 1 – has not been evaluated. As a result of the expected higher temperature difference in W-FG-EVAP no reduction of exergy destruction would be achieved. In case 2 a side stream of potassium, with a higher pressure than in W-K-SH1, is used in W-K-SH2 and W-K-RH2 to further superheat and reheat the water up to a temperature of 570 °C. Figure 4 illustrates this approach. The exergy destruction rate decreases by 3.2 MW in the superheater and reheater subsystem for case 2. Finally, this improvement strategy yields to the overall highest net efficiency.

4 Conclusions

Binary Rankine cycles are lead to increases in the efficiency of energy conversion processes. This paper presents the exergy analysis of a coal-fired binary Rankine cycle with potassium and water as working fluids including the flue gas streams in the steam generator. Three different cases were considered. A design analysis as well as sensitivity studies show the effects of stream combinations and key parameters on the net amount of power and the overall exergy destruction rate. The energetic efficiencies are higher than 50 %, whereas the exergetic efficiencies lie between 46.9 and 47.8 %. In future research, the part-load performance will be studied and exergoeconomic analyses as well as a mathematical optimization of the process will be conducted. Furthermore, the pinch analysis could help to improve the process.

[22] Weighted average of the specific work over all stages, e.g. for reference. K-ST-1…K-ST-6: w_K = 118 kJ/kg. W-HPT, W-IPT, W-LPT: w_W = 179 kJ/kg.

[23] E.g. for Reference. K-ST-1…K-ST-6: ϵ_K = 93.9 %. W-HPT, W-IPT, W-LPT: ϵ_W = 90.1 %

Nomenclature

The short names of the components are combinations of the following abbreviations. For heat exchangers with different fluids the primary side is named first. So W-K-RH2 means the second water-potassium-reheater; water is primary, potassium is secondary.

Abbreviations

APH*n*	Air preheater
CC	Combustion chamber
COND	Condenser
CW, FW	Cooling water, feed water
DEARATOR	Dearator and feed water tank
ECO, EVAP, SH*n*,RH*n*	Economizer, evaporator, superheater, reheater
ESP	Electrostatic precipitator
FD-FAN, ID-FAN, PUMP	Forced draft fan, induced draft fan, pump
FG, K, W	Flue gas, potassium, water
FGD	Flue gas desulfurisation
HP, LP, PH-*n*	High-pressure, low-pressure, preheater
HPT, IPT, LPT	Steam turbine; water; high,- intermediate-, low-pressure
SCR	Selective catalytic reduction
ST-*n*	Steam turbine; potassium; *n*th-stage

Letter symbols

$\dot{E}$	Exergy rate	W
h	Specific enthalpy	J/kg
$\dot{H}$	Enthalpy rate	W
$\dot{m}$	Mass flow rate	kg/s
LHV	Lower heating value	J/kg
p	Pressure	bar
$\dot{S}$	Entropy rate	W/K
T	Temperature	°C
$\dot{W}$	Work rate	W
x	Molar fraction of substance	mol/mol
y	Exergy destruction ratio, exergy loss ratio	–

Greek symbols

Δ	Difference	–
ϵ	Exergetic efficiency	–
η	Efficiency	–
ξ	Mass fraction of substance	kg/kg

Subscripts and superscripts

0	Reference state
D, F, L, P	Destruction, fuel, loss, product
CH	Chemical
e	Exit
el, m	Electrical, mechanical
gen	Generation
min	Minimum
net, tot	Net amount, total amount
prim, sec	Primary, secondary
s	Isentropic

References

[1] Emmet WLR. Power from mercury vapor. Trans AIEE. 1913;32:2133–2149.

[2] Emmet WLR. The Emmet Mercury-Vapor Process. Trans ASME. 1924;46:253–285.

[3] Emmet WLR. Status of the Emmet Mercury-Vapor Process. Mech Eng. 1937;59:840.

[4] Birnbaum U, Bongartz R, Linssen J, Markewitz P, Vögele S. Energietechnologien 2050. Jülich: Institut für Energieforschung; 2010. German.

[5] Moran MJ, Shapiro HN. Fundamentals of Engineering Thermodynamics. 5th ed. Chichester, West Sussex: Wiley; 2006.

[6] Fraas AP. A potassium-steam binary vapor cycle for a molten-salt reactor power plant. Trans ASME, J Eng Power. 1966;88(4):355–366.

[7] Fraas AP. A potassium-steam binary vapor cycle for better fuel economy and reduced thermal pollution. Trans ASME, J Eng Power. 1973;95(1):53–63.

[8] Zipkin MA, Schnetzer E. Design Compromises in Space Power Systems. In: Hecht F, editor. Xth International Astronautical Congress London 1959. Berlin: Springer; 1960. pp. 560–575.

[9] Ewing CT, Stone JP, Spann JR, Miller RR. High temperature properties of potassium. J Chem Eng Data. 1966;11(4):460–467.

[10] Foust OJ, editor. Sodium-NaK Engineering Handbook. vol. 1: Sodium Chemistry and Physical Properties. New York: Gordon and Breach; 1972.

[11] Collier JG, Cox RF, Evans LS, Bainbridge GR. Potassium/steam cycle for a high efficienty gas-cooled reactor power station. Electrical Review. 1974;195(16):565–568.

[12] Ganic E, Seider WD. Computer simulation of potassium-steam combined-cycle, electrical power plants. Comput Chem Eng. 1977;1(3):161–169.

[13] Rajakovics GE. Extrem hohe Kraftwerkswirkungsgrade durch Dreifach-Dampfprozeß. ÖZE. 1974;27(4):102–126. German.

[14] Brockel D. Der Dreifachdampfprozeß. VGB-Kraftwerkstechnik. 1984;64(3):201–210. German.

[15] von Lojewski D, Jansing W. Der Zweifachdampfprozeß: Ein wirtschaftliches Konzept der Zukunft? VGB-Kraftwerkstechnik. 1989;69(2):138–147. German.

[16] Urban H, Haneke R, von Lojewski D, Mair R, Pannen H, Schiemann W, et al. Entwicklung eines Zweifach-Dampfprozesses mit Kalium- und Wasser-/Dampfkreislauf für Kohlekraftwerke (BRC Projekt). Oberhausen: Deutsche Babcock Werke; 1988. German.

[17] Teubner H. Entwicklung eines Zweifach-Dampfprozesses mit Kalium- und Wasser-/Dampfkreislauf – Teil 1: Kaliumtechnologie. Bergisch Gladbach: Siemens; 1992. German.

[18] Angelino G, Invernizzi C. Binary and ternary liquid metal-steam cycles for high-efficiency coal power stations. Proc IMechE, Part A: J Power and Energy. 2006;220(3):195–205.

[19] Saunderson DJ, Budiman RA. Analysis of binary cycle efficiency using Redlich-Kwong equation of state. Proc IMechE, Part A: J Power and Energy. 2011;225:567–578.

[20] Woudstra N, Woudstra T, Pirone A, van der Stelt T. Thermodynamic evaluation of combined cycle plants. Energy Convers Manage. 2010;51(5):1099–1110.

[21] Effenberger H. Dampferzeugung. Berlin: Springer; 2000. German.

[22] Eisermann W, Johnson P, Conger WL. Estimating thermodynamic properties of coal, char, tar and ash. Fuel Process Technol. 1980;3(1):39–53.

[23] Bakshi BR, Gutowski TG, Sekulić DP, editors. Thermodynamics and the destruction of resources. New York: Cambridge University Press; 2011.

[24] Singer JG. Combustion fossil power. 4th ed. Windsor (US-CT): Combustion Engineering; 1991.

[25] Bejan A, Tsatsaronis G, Moran M. Thermal design and optimization. New York: J. Wiley; 1996.